Japanese Journal of Applied Physics
Vol. 47, No. 4, 2008, pp. 3156–3161

Interface Control by Surface-Initiated Deposition Polymerization and Its Application to Organic Light-Emitting Devices

Akira KAWAKAMI[1,2], Kiyoi KATSUKI[1], Rigoberto C. ADVINCULA[3], Kuniaki TANAKA[1], Kenji OGINO[1], and Hiroaki USUI[1*]

[1]*Tokyo University of Agriculture and Technology, Koganei, Tokyo 184-8588, Japan*
[2]*Konica Minolta Technology Center, Inc., Hino, Tokyo 191-8511, Japan*
[3]*University of Houston, 136 Fleming Building, Houston, TX 77204-5008, U.S.A.*

(Received October 1, 2007; accepted December 17, 2007; published online April 25, 2008)

Surface-initiated deposition polymerization was applied to the preparation of a hole transport layer (HTL) on an indium–tin oxide (ITO) electrode. A silane-based self-assembled monolayer (SAM) that has an azo terminal group was prepared on an ITO surface on which a vinyl monomer of carbazole (CPA) or tetraphenyldiaminobiphenyl (vTPD) was deposited by physical vapor deposition. The polymerization of the HTL was achieved by electron-assisted deposition. UV irradiation, as well as conventional evaporation, was not capable of growing polymer films on the SAM. Organic light-emitting diodes (OLEDs) were prepared by depositing tris(8-quinolinolato) aluminum (Alq_3) on the HTL. The surface-initiated deposition polymerization was effective in markedly increasing device current flow and reducing turn-on voltage. However, luminescence efficiency was not improved by this method owing to improper carrier balance under excessive hole injection. Nevertheless, surface-initiated deposition polymerization was effective in improving film morphology, stability, and hole injection characteristics. [DOI: 10.1143/JJAP.47.3156]

KEYWORDS: organic light-emitting diode, OLED, organic EL, deposition polymerization, self-assembled monolayer, SAM, surface-initiated polymerization

1. Introduction

After the pioneering work by Tang *et al.*,[1)] organic light-emitting diodes (OLEDs) have attained remarkable development in materials and device structures. High-performance devices have been realized by constructing multilayer structures by the vapor deposition of small organic molecules. However, one of the remaining problems is the insufficient device durability, which is inherent to small molecules that have low glass transition temperatures. In this respect, polymer LEDs[2)] are expected to have excellent thermal and mechanical stabilities. Such polymer devices also have advantages in mass production by wet coating. However, polymers are not convenient for constructing multilayered structures that are essential for achieving high luminescence efficiency. To solve these problems, the authors have proposed the use of vapor deposition polymerization that enables the formation of polymeric thin films by the physical vapor deposition of small molecules.[3,4)] Electron-assisted deposition is particularly useful for polymerizing acrylate or vinyl monomers. Deposition polymerization is effective in improving film stability, and has been applied to OLED construction.[5,6)]

Another problem inherent to organic devices is instability and imperfections at the film/substrate interface. Unlike epitaxially grown inorganic thin films, most organic films only physically adsorb on substrate surfaces without forming strong chemical bonds at the interface. This leads to a charge injection barrier at the interface as well as to the insufficient adhesion strength of organic films to substrates. The authors have shown that the interface stability can be improved by surface-initiated deposition polymerization, which combines vapor-deposition polymerization with the use of a self-assembled monolayer (SAM) that has a polymerization initiator.[7)] The SAM layer plays a role in binding the deposited film to the substrate as well as in initiating the polymerization of monomers deposited on its surface. In our previous study, 3-(*N*-carbazolyl)propyl acrylate (CPA) was deposited on a thiole SAM that was formed on a Au substrate. The SAM had an azo terminal group that initiates the polymerization of CPA upon irradiation with ultraviolet (UV) light. The films formed by this method had excellent thermal stability compared with conventionally evaporated monomer films. This result suggests that surface-initiated deposition polymerization is a promising film deposition technique for constructing OLEDs.

From the viewpoint of OLEDs, SAMs have been reported to be effective buffer layers between an indium–tin oxide (ITO) anode and a hole transport layer (HTL).[8,9)] It is considered that a SAM forms an interface dipole layer, which lowers the charge injection energy barrier from ITO to HTL.[10)] SAMs also work to block chemical reactions[11)] or moisture penetration.[12)] They improve the wettability of HTL on an ITO surface[13)] and assist in forming pinhole-free layers.[14)] On the other hand, there have been no studies that used SAMs as polymerization initiators to form covalent bonds between an ITO anode and an organic layer.

The above technological background, including the concepts of electron-assisted deposition polymerization, surface-initiated deposition polymerization, and the SAM buffer layer, led to the idea that the surface-initiated deposition polymerization of HTL on an ITO surface might be an effective solution to the problems of the thermal and interfacial instabilities of OLED. In this study, we investigate the effect of surface-initiated deposition polymerization on the device characteristics of OLED. A silane-based SAM that has an azo terminal group was prepared on an ITO surface, on which acrylate or vinyl monomers were evaporation-deposited to form HTL. UV irradiation or electron-assisted deposition was employed to enhance polymerization. The OLED characteristics were compared for devices constructed with and without an initiator SAM layer.

*E-mail address: usui@cc.tuat.ac.jp

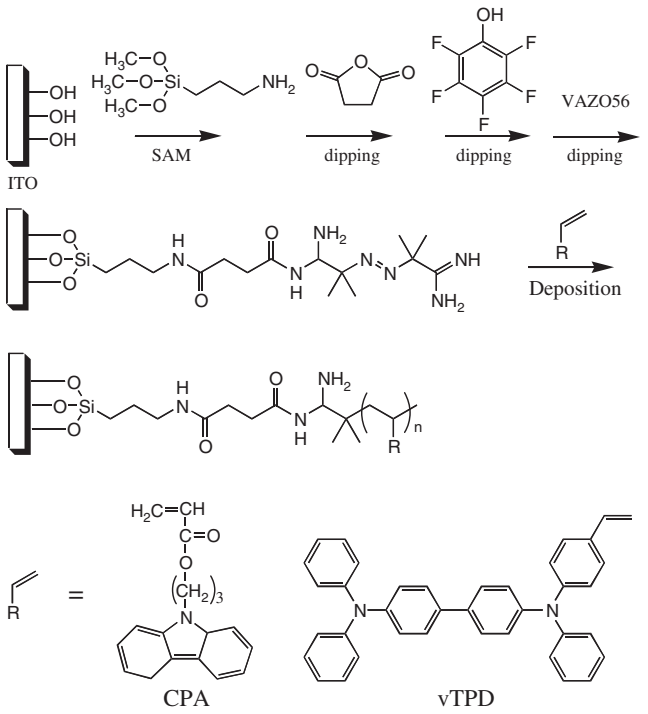

Fig. 1. Film formation scheme by surface-initiated deposition polymerization on ITO substrate. The first line represents the formation of SAM that has an azo terminal group. The second and third lines correspond to the vapor deposition polymerization process. The chemical structures of the evaporated monomers are shown in the last line.

2. Experimental Procedure

Figure 1 shows the scheme of film formation carried out in this study. The film formation process consists of two stages, SAM formation and physical vapor deposition. In the first stage, a SAM was prepared on an ITO substrate by the following procedure.[15] An ITO-coated glass substrate was immersed in a mixture of aqueous ammonia, hydrogen peroxide, and pure water (volume ratio 1 : 1 : 5) at 60 °C for 1 h. After drying at 100 °C for 12 h, the substrate was processed in a UV-ozone cleaner (Filgen UV253) for 15 min. The cleaned substrate was immersed in a toluene solution of 0.5 mM (3-aminopropyl)triethoxysilane (APS) overnight at room temperature. The APS-functionalized substrate was immersed in 35 mL of *N*,*N*-dimethylformamide (DMF) solution containing 3.5 g of succinic anhydride and 0.35 g of 4-(dimethylamino)pyridine for 18 h. The substrate was then immersed in an ethanol solution containing 0.1 M 1-ethyl-3-(3-dimethylaminopropyl)-carbodiimide hydrochloride and 0.2 M pentafluorophenol for 45 min. At this point, surface functionalization was confirmed from the extremely high hydrophobicity of the substrate. In the last step, the substrate was immersed in a methanol solution containing 10 mM Vazo 56 (DuPont) for 1 h. Each immersion step was followed by thorough rinsing and ultrasonic cleaning with the appropriate solvents.

The second stage of film formation was the physical vapor deposition of HTL monomers on the SAM-modified ITO surface. As the HTL monomer, CPA or *N*,*N*,*N*′-triphenyl-*N*′-(4-vinylphenyl)-biphenyl-4,4′-diamine (vTPD) was employed. The deposition was achieved in a high-vacuum chamber at a background pressure of 1×10^{-3} Pa by either conventional evaporation or electron-assisted deposition. Details of the electron-assisted deposition have been described elsewhere.[6] CPA and vTPD were evaporated at 100 and 300 °C, respectively, yielding a deposition rate of 0.5 nm/min. CPA or vTPD was deposited to a thickness of 50 nm. Film thickness was monitored with a quartz crystal microbalance that had been calibrated with a surface profilemeter (Sloan DEKTAK 2A).

For electron-assisted deposition, monomer vapor was irradiated with electrons of 10 mA. The effect of UV irradiation was also examined to enhance the solid-phase polymerization of HTL. For this purpose, the HTL film was transferred to another high-vacuum chamber and exposed to UV light from a high-pressure mercury lamp. The irradiation was achieved for 3 h at 0.3 mW/cm^2. The deposited films were characterized using their infrared (IR) absorption spectra measured in the reflection-absorption mode on an ITO surface at an incidence angle of 80°. Film morphology was examined by differential interference optical microscopy. To confirm the binding of the films to the substrate, the films deposited on bare and SAM-modified ITO surfaces were immersed in tetrahydrofuran (THF) and observed by atomic force microscopy (AFM).

For OLED fabrication, the ITO layer was patterned in 2-mm-wide stripes, and 50-nm-thick HTLs were deposited as stated above with and without SAM modification. The specimen was transferred to another vacuum chamber, where a 50-nm-thick tris(8-quinolinolato) aluminum (Alq_3) emissive layer, a 0.5-nm-thick lithium fluoride injection layer, and a 200-nm-thick aluminum cathode were evaporation-deposited successively. The active device area was 2×2 mm^2. The device was operated in air at a constant driving voltage, increasing stepwise at a voltage step of 1 V for a duration of 30 s until the device broke down.

3. Results and Discussion

3.1 Deposition polymerization of CPA

In our previous study,[7] we have shown that CPA films deposited on an azo-functionalized SAM layer on Au surfaces can be polymerized by postdeposition UV irradiation. The IR spectrum of the UV-polymerized CPA on Au/SAM was reproduced in Fig. 2(b), together with the spectrum of the CPA monomer (a). The spectrum of CPA is characterized by the CH_2 in-plane deformation (1408 cm^{-1}) and C–H in-plane deformation (1297 cm^{-1}) of the vinyl group. In addition, a stretching band of the C=O group, which is adjacent to the vinyl group, appears at 1717 cm^{-1}; this represents an unsaturated ester. When CPA was evaporated on Au/SAM followed by UV irradiation, the bands of the vinyl group disappeared, and the C=O stretching band shifted to 1734 cm^{-1}, representing a saturated ester. These changes indicate the vinyl polymerization of CPA. The spectra of the as-deposited and UV-irradiated CPA films prepared on ITO/SAM in this study are shown Figs. 2(c) and 2(d), respectively. The as-deposited film (c) clearly showed absorptions by the vinyl group, indicating that the film is mostly in the monomer state. After the UV irradiation (d), the vinyl peaks reduced their intensity, but were still detectable. In addition, the shift of the C=O band was not as complete as that observed with the film on Au/SAM (b). Figure 3 shows differential interference micro-

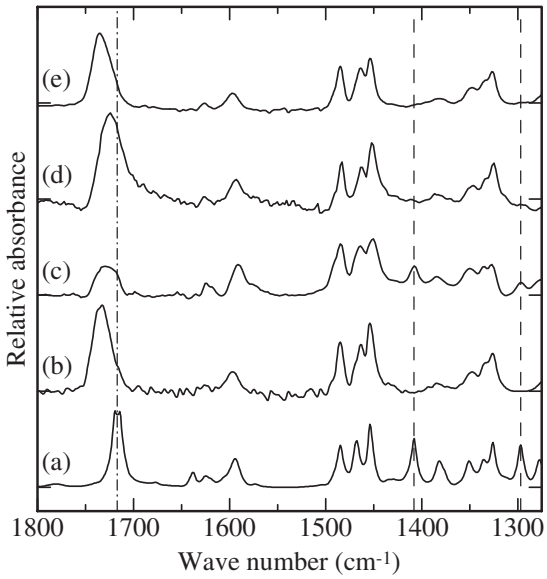

Fig. 2. IR absorption spectra of CPA monomer (a), UV-irradiated film on Au/SAM (b), as-deposited (c), and UV-irradiated (d) films on ITO/SAM, and the film by electron-assisted deposition on ITO/SAM (e).

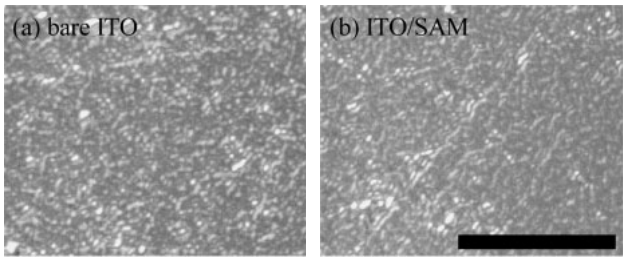

Fig. 3. Differential interference micrographs of as-deposited CPA film on bare ITO (a) and UV-irradiated film on ITO/SAM (b). The deposition was achieved by conventional evaporation. The scale bar corresponds to a length of 50 μm.

graphs of an as-deposited CPA film on bare ITO (a) and a UV-irradiated film on ITO/SAM (b). As is mostly the case in the conventional vapor deposition of small molecules, the simply evaporated film on a bare ITO surface (a) showed a polycrystalline structure consisting of small grains. The UV-irradiated film on ITO/SAM (b) assumed almost the same structure. These results suggest that the polymerization on ITO/SAM does not proceed as efficiently as that on Au/SAM with UV irradiation.

To further enhance polymerization, electron-assisted deposition was employed instead of the simple evaporation. Figure 2(e) shows the IR spectrum of the film deposited on ITO/SAM by the electron-assisted method. This spectrum represents the as-deposited film, and the following UV irradiation did not cause an additional change. By the electron-assisted deposition, vinyl absorption mostly disappeared, and the C=O band showed clear shift to the position of a saturated ester. This result suggests that polymerization on ITO/SAM can be enhanced by electron-assisted deposition.

It is expected that the SAM plays a role in binding the overlying film to the substrate as well as in initiating the polymerization. To confirm the binding of CPA to the substrate, the films polymerized on the bare and SAM-

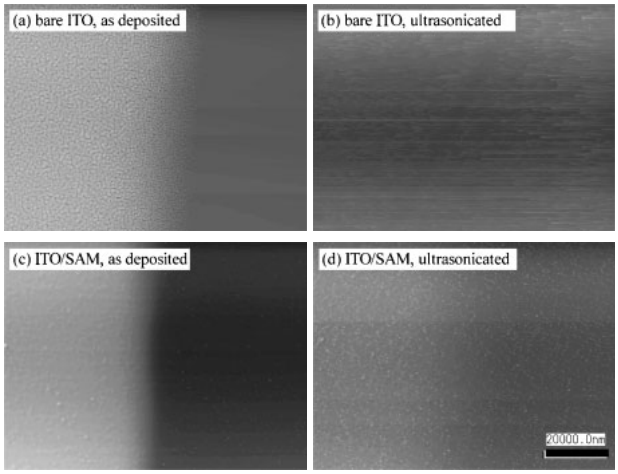

Fig. 4. AFM images of deposition-polymerized CPA films on bare (a and b) and SAM-modified (c and d) ITO surfaces before (a and c) and after (b and d) ultrasonication in THF for 5 min. The images show edges of the films revealing film thicknesses. The left half in an image represents the film and the right half the substrate surface. The scale bar corresponds to a length of 20 μm.

modified ITO surfaces were ultrasonicated in THF for 5 min at room temperature, and observed by AFM. In this case, 200-nm-thick films were prepared at a deposition rate of 2 nm/min. Figure 4 shows the AFM images of the films deposited on bare (a and b) and SAM-modified (c and d) ITO surfaces before (a and c) and after (b and d) ultrasonication in THF. The edges of the films were observed to measure film thickness from step height. On the bare ITO surface, the film completely dissolved in THF by 5 min ultrasonication. On the other hand, the film deposited on the SAM did not dissolve in THF completely but only reduced its thickness to 130 nm. This result suggests that part of the CPA molecules on the SAM-modified ITO are chemically bound to the substrate surface. The film on the bare ITO surface was analyzed by gel permeation chromatography (GPC) after dissolving in THF. It was found that the film formed by the electron-assisted deposition contained polymers with a number-averaged molecular weight of 140,000 and a fraction of 84%. The film polymerized on the SAM was difficult to analyze by GPC due to its insufficient solubility.

The electron-assisted deposition gave a prominent effect on film morphology. Figure 5 shows the CPA films deposited by the electron-assisted method on the bare (a, b) and SAM-modified (c, d) ITO surfaces before (a, c) and after (b, d) UV irradiation. Unlike the films deposited by simple evaporation shown in Fig. 3, the films prepared by electron-assisted deposition had smooth and uniform morphology especially when the ITO surface was modified with the SAM. These results indicate that the surface-initiated deposition polymerization by the combined use of an initiator SAM with electron-assisted deposition enables the formation of uniform polymer films. When electron-assisted method was employed, the postdeposition UV irradiation did not seem to bring any further difference in film morphology.

The reason polymerization behavior differed between the SAMs on the Au and ITO surfaces is not clear at this point. It is reported that the reproducible formation of dense monolayers on an ITO is rather difficult compared to that on

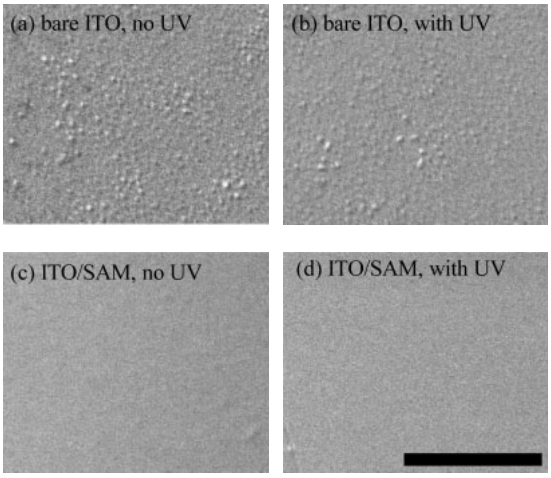

Fig. 5. Differential interference micrographs of CPA films deposited on bare ITO (a, b) and ITO/SAM (c, d) by electron-assisted method. The films prepared without (a, c) and with (b, d) UV irradiation are shown. The scale bar corresponds to a length of 50 μm.

a Au surface, where thiole molecules can form densely packed monolayers.[16] As a consequence, the number density of azo initiators on the Au surface is expected to be high enough to drive film growth by surface-initiated polymerization, whereas the initiator density on ITO is not, and radicals need to be supplied from an additional source such as electron irradiation. This hypothesis is supported by the fact that the film polymerized on the ITO surface is partly soluble in THF, while that polymerized on the Au has poor solubility.[7] However, the improvement in film morphology achieved by introducing the SAM suggests that SAM molecules play a role in anchoring the deposited film to the substrate.

3.2 *OLED with CPA hole transport layer*

From the results in the previous section, OLEDs were fabricated on the bare and SAM-modified ITO surfaces by depositing CPA films by the electron-assisted method for HTLs. The effect of postdeposition UV irradiation was also examined. Figure 6 shows the current–voltage and luminance–voltage characteristics for the four different fabrication conditions combining with/without the SAM and with/without UV irradiation. Regardless of UV irradiation, the SAM-modification led to a notable increase in device current and a significant decrease in turn-on voltage. This result is consistent with the improvement in film morphology shown in Fig. 5. However, the effect of postdeposition UV irradiation was not straightforward. On the bare ITO surface, turn-on voltage was slightly reduced by UV irradiation, whereas that on SAM-modified ITO surface was increased by UV irradiation. The authors do not have sufficient information to explain the effect of postdeposition UV irradiation. Presumably, UV light can have contradictory effects of initiating polymerization and damaging organic molecules. However, it can be concluded that UV irradiation is not necessary from the standpoints of both polymerization and device fabrication as long as electron-assisted deposition is employed.

Unfortunately, the maximum luminance observed before the device breakdown was not improved by the surface-initiated deposition polymerization because the increase in device current caused a larger power dissipation. Such a marked enhancement of hole injection also affects carrier balance. As a consequence, luminescence efficiency was not improved by the use of the SAM-modified surface. Without UV irradiation, the power efficiency was 0.42 lm/W on the bare ITO surface, which decreased to 0.23 lm/W on the SAM-modified ITO surface. After driving the OLEDs with a stepwise increase in voltage until they broke down, the devices were observed by differential interference microscopy from the back of substrate through the ITO electrode. Figure 7 shows the images of the devices prepared on the bare ITO surfaces (a, b) and on the SAM-modified ITO srufaces (c, d) without (a, c) and with (b, d) the postdeposition UV irradiation. The device on the bare ITO surface was damaged in the whole device area, while the device prepared on the SAM-modified ITO surface was damaged only in localized regions. This result suggests that surface-initiated deposition polymerization is effective not only for enhancing current injection but also for improving the physical robustness of films. Although the effect of UV irradiation was not straightforward in polymerization and device characteristics, UV irradiation appeared to reduce the irregularities caused by the device damage, as shown in Fig. 7(d).

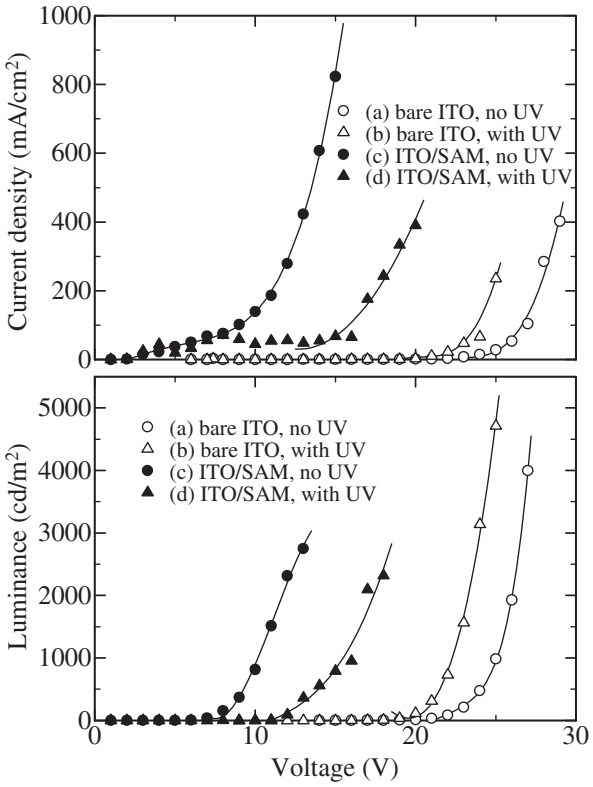

Fig. 6. Current–voltage (upper) and luminance–voltage (lower) characteristics of OLEDs having CPA HLTs by electron-assisted deposition. The devices were prepared on bare (a, b) and SAM-modified (c, d) ITO surfaces without (a, c) and with (b, d) postdeposition UV irradiation.

3.3 *OLED with vTPD hole transport layer*

The surface-initiated deposition polymerization on ITO can be applied to the preparation of various materials that have polymerizable groups like vinyl or acrylate monomers.

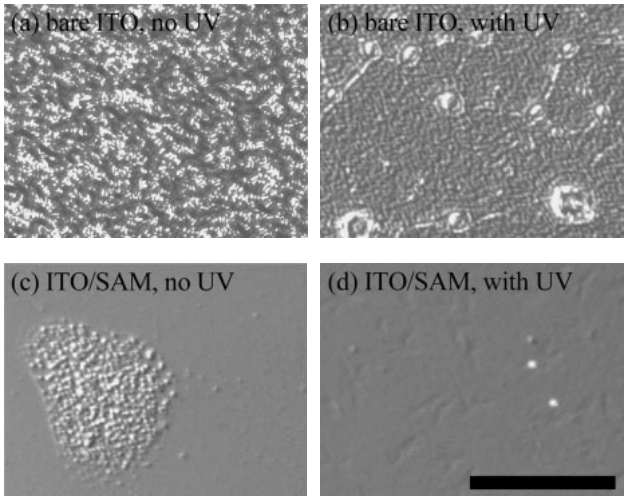

Fig. 7. Differential interference micrographs of OLED observed through the substrate back after driving the devices until the devices break down. CPA layers were deposited on bare ITO (a, b) and on ITO/SAM (c, d) by electron-assisted method without (a, c) and with (b, d) the postdeposition UV irradiation. The scale bar corresponds to a length of 50 μm.

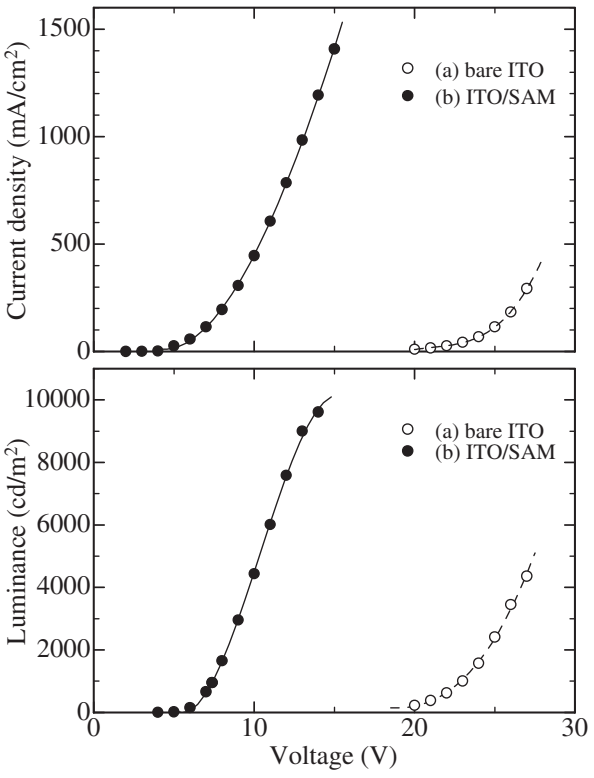

Fig. 8. Current–voltage (upper) and luminance–voltage (lower) characteristics of OLEDs having vTPD HTLs by electron-assisted deposition. The devices were prepared on bare (a) and SAM-modified (b) ITO surfaces without postdeposition UV irradiation.

OLEDs were fabricated using the same procedure described in the previous section using a vTPD hole transport material instead of CPA. Their current–voltage and luminance voltage characteristics are shown in Fig. 8. In good correspondence with that in the case of CPA, the surface-initiated polymerization led to a marked increase in device current and a decrease in turn-on voltage. A luminance as high as 10000 cd/m^2 was obtained with this simple two-layer device. However, the power efficiency was 0.34 lm/W in either case, and was not improved in spite of the lowering of turn-on voltage of the SAM-modified device. To improve power efficiency, electron injection from the cathode also needs to be enhanced so as to match the increase in the hole current from ITO. The devices that were damaged after the breakdown was observed by differential interference microscopy through the substrate back, as shown in Fig. 9. Without the SMA layer, the damage was observed as extensive film delamination, whereas the damage was limited to certain spots when the HTL was deposited by the surface-initiated polymerization.

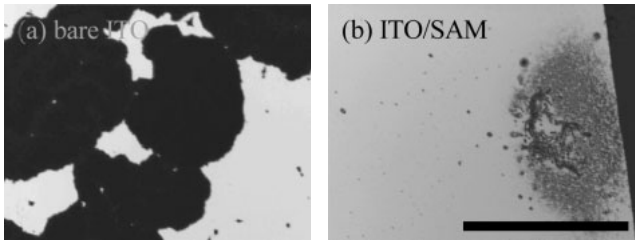

Fig. 9. Differential interference micrographs of OLED using vTPD HTLs observed from substrate back after breakdown of devices. The vTPD films were deposited on the bare (a) and SAM-modified (b) ITO surfaces by electron-assisted method without postdeposition UV irradiation. The scale bar corresponds to a length of 50 μm.

4. Conclusions

Surface-initiated deposition polymerization was employed in preparing HTLs on ITO substrates. For this purpose, a SAM layer that has an azo terminal group was prepared on an ITO surface, on which carbazole monomer CPA was deposited by physical vapor deposition. The polymerization of CPA was achieved by electron-assisted deposition, whereas UV irradiation, as well as conventional evaporation, was not effective in initiating polymer growth. Flat and uniform thin films were obtained by the surface-initiated deposition polymerization, while the films consisting of monomers have a granular structure.

Simple OLED devices were prepared by evaporating Alq_3 on the CPA layer. The surface-initiated deposition polymerization was effective in markedly increasing device current and decreasing turn-on voltage. However, luminescence efficiency was not improved by this method, probably due to improper carrier balance caused by the excessive increase of hole injection through the SAM-modified surface. OLEDs were also fabricated using vTPD as a monomer for HTL, resulting in a similar reduction in turn-on voltage when deposited by the surface-initiated polymerization.

As far as the effect of SAM is concerned, the number density of the polymerization initiator formed by self-assembly appeared to be smaller on the ITO surface than on the Au surface. However, the initiator SAM molecules efficiently played a role in anchoring the organic layer to the ITO surface, and in improving film morphology, thermal stability and adhesion strength. In conclusion, surface-initiated deposition polymerization can be a promising technique for fabricating thin-film organic devices on inorganic substrates.

Acknowledgement

This research was supported by a Grant-in-Aid for Scientific Research No. 16350097 from the Japan Society for the Promotion of Science.

1) C. W. Tang and VanSlyke: Appl. Phys. Lett. **51** (1987) 913.
2) J. H. Burroughes, D. D. C. Bradley, A. R. Brown, N. Marks, K. Mackay, R. H. Friend, P. L. Burns, and A. B. Holms: Nature **347** (1990) 539.
3) H. Usui: Thin Solid Films **365** (2000) 22.
4) H. Usui: IEICE Trans. Electron. **E83-C** (2000) 1128.
5) M. Tamada, H. Koshikawa, T. Suwa, T. Yoshioka, H. Usui, and H. Sato: Polymer **41** (2000) 5661.
6) K. Katsuki, A. Kawakami, K. Ogino, K. Tanaka, and H. Usui: Jpn. J. Appl. Phys. **44** (2005) 4182.
7) K. Katsuki, H. Bekku, A. Kawakami, J. Locklin, D. Patton, K. Tanaka, R. Advincula, and H. Usui: Jpn. J. Appl. Phys. **44** (2005) 504.
8) F. Nüesch, L. Si-Ahmed, B. François, and L. Zuppiroli: Adv. Mater. **9** (1997) 222.
9) I. H. Campbell, J. D. Kress, R. L. Martin, D. L. Smith, N. N. Barashkov, and J. P. Feraris: Appl. Phys. Lett. **71** (1997) 3528.
10) S. F. J. Appleyard, S. R. Day, R. D. Pickford, and M. R. Willis: J. Mater. Chem. **10** (2000) 169.
11) K. W. Wong, H. L. Yip, Y. Luo, K. Y. Wong, W. M. Lau, K. H. Low, H. F. Chow, Z. Q. Gao, W. L. Yeung, and C. C. Chang: Appl. Phys. Lett. **80** (2002) 2788.
12) B. Choi, J. Rhee, and H. H. Lee: Appl. Phys. Lett. **79** (2001) 2109.
13) C.-C. Hsiao, C.-H. Chang, M.-C. Hung, N.-J. Yang, and S.-A. Chena: Appl. Phys. Lett. **86** (2005) 223505.
14) J. E. Malinsky, G. E. Jabbour, S. E. Shaheen, J. D. Anderson, A. G. Richter, T. J. Marks, N. R. Armstrong, B. Kippelen, P. Dutta, and N. Peyghambarian: Adv. Mater. **11** (1999) 227.
15) J. Hyun and A. Chilkoti: Macromolecules **34** (2001) 5644.
16) S.-Y. Oh, Y.-J. Yun, K.-H. Hyungyb, and S.-H. Han: New J. Chem. **28** (2004) 495.